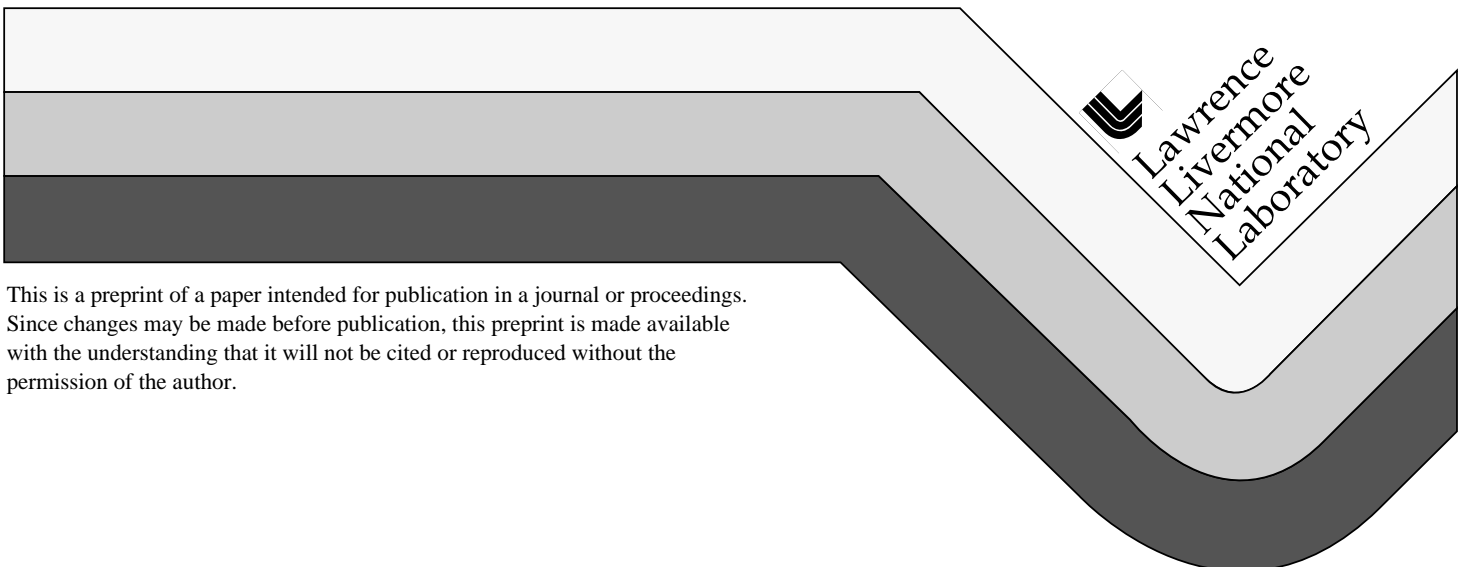


Grain and Burnup Dependence of Spent Fuel Oxidation: Geological Repository Impact

E.J. Kansa
B.D. Hanson
R.B. Stout

This paper was prepared for submittal to the
Materials Research Society 1998 Fall Meeting
Boston, MA
November 30-December 4, 1998

October 15, 1998



This is a preprint of a paper intended for publication in a journal or proceedings.
Since changes may be made before publication, this preprint is made available
with the understanding that it will not be cited or reproduced without the
permission of the author.

DISCLAIMER

This document was prepared as an account of work sponsored by an agency of the United States Government. Neither the United States Government nor the University of California nor any of their employees, makes any warranty, express or implied, or assumes any legal liability or responsibility for the accuracy, completeness, or usefulness of any information, apparatus, product, or process disclosed, or represents that its use would not infringe privately owned rights. Reference herein to any specific commercial product, process, or service by trade name, trademark, manufacturer, or otherwise, does not necessarily constitute or imply its endorsement, recommendation, or favoring by the United States Government or the University of California. The views and opinions of authors expressed herein do not necessarily state or reflect those of the United States Government or the University of California, and shall not be used for advertising or product endorsement purposes.

Grain and burnup dependence of spent fuel oxidation: Geological repository impact

E.J. Kansa*, B.D. Hanson**, and R.B. Stout*

* Earth and Environmental Sciences Directorate
Lawrence Livermore National Laboratory
Livermore, CA 94551-9900

** Pacific Northwest National Laboratory
PO Box 999, Mail Stop P7-27
Richland, WA 99352

ABSTRACT

Further refinements to the oxidation model of Stout et al. have been made. The present model incorporates the burnup dependence of the oxidation rate in addition to an allowance for a distribution of grain sizes. The model was tested by comparing the model results with the oxidation histories of spent fuel samples oxidized in Thermogravimetric Analysis (TGA) or Oven Dry-Bath (ODB) experiments. The comparison between the experimental and model results are remarkably close and confirm the assumption that grain-size distributions and activation energies are the important parameters to predicting oxidation behavior. The burnup dependence of the activation energy was shown to have a greater effect than decreasing the effective grain size in suppressing the rate of the reaction $U_4O_9 \rightarrow U_3O_8$. Model results predict that U_3O_8 formation of spent fuels exposed to oxygen will be suppressed even for high burnup fuels that have undergone restructuring in the rim region, provided the repository temperature is kept sufficiently low.

INTRODUCTION

Oxidation of UO_2 to U_3O_8 is a concern in a geological repository, such as the potential site at Yucca Mountain, since the 30-36% increase in volume as the fuel oxidizes can potentially stress the cladding. Such stresses are sufficient to split the cladding [1] and may result in direct contact of the fuel with water. U_3O_8 has also been shown to dissolve more readily than UO_2 [2]. Experimental and modeling efforts have been underway to determine the oxidation response of spent fuel under repository conditions.

Spent (irradiated) fuel refers to UO_2 that has undergone fission in nuclear reactors. As a result, the UO_2 is chemically and physically altered from the original unirradiated fuel. For every atom undergoing fission, nearly two fission product atoms are produced. Even though the concentration of these "impurity" atoms is relatively small, it has been shown that the oxygen potential of the fuel changes, at least initially, with burnup [3]. The thermal stress to which the fuel is subjected results in radial and axial cracking. Also, when the pellet-averaged burnup exceeds a threshold of 40-50 MWd/kgM, the fuel grains undergo a marked restructuring, producing a very porous rim region where the grains have experienced a 1000 to 10000 fold grain volume reduction, (see Walker et al. [4]).

A review [5] of the literature shows that, with respect to oxidation, spent fuel behaves sufficiently different from unirradiated UO_2 . Unirradiated fuel has been shown to oxidize following the sequence $UO_2 \rightarrow U_3O_7 \rightarrow U_3O_8$ whereas spent fuel oxidizes as $UO_2 \rightarrow U_4O_9 \rightarrow U_3O_8$. Also, for spent fuels of sufficient burnup and at moderate temperatures, no U_3O_8 has been observed until after conversion of the UO_2 to U_4O_9 is complete. This initial conversion usually occurs at a change in the oxygen-to-metal ratio, $\Delta(O/M)$, of about 0.42, which corresponds to the time $t_{2.4}$. Spent fuel typically has shown a resistance to further oxidation, exhibited as a plateau on a plot of the O/M ratio as a function of time. Oxidation to U_3O_8 then proceeds to completion at a nominal O/M ratio of about 2.75. Such plateau behavior is not observed in the oxidation of UO_2 at similar temperatures.

The soluble fission products, whose concentrations are proportional to burnup, and the higher actinides behave as dopants that inhibit the oxidation of U_4O_9 to U_3O_8 , (see McEachern et al.[7]). The time required for onset of U_3O_8 formation, as well as the rate at which U_3O_8 is formed has been shown [5] to be dependent on burnup. The activation energy for the U_4O_9 to U_3O_8 transition was modeled as linearly dependent on burnup and follows the equation

$$E_A = E_{A0} + \alpha B \quad (1)$$

where E_A is the total activation energy for the conversion of U_4O_9 to U_3O_8 (kJ/mol); E_{A0} is the temperature-dependent activation energy, which was determined to be approximately 155 kJ/mol (in excellent agreement with literature values found for unirradiated fuel [6,7]); α is the coefficient for burnup-dependence, nominally 1.2 kJ/mol per MWd/kg M; and B is the burnup (MWd/kg M). Uncertainties of at least 10% were found for both E_{A0} and α . Also, it should be emphasized that burnup is only an approximate measure of the total soluble impurity concentration which dictates oxidation behavior; a detailed discussion is presented by Hanson [5].

Finally, as the fuel oxidizes from UO_2 to the denser U_4O_9 , the grains contract, opening the grain boundaries. However, some of the stress of this phase transition is accommodated by cracking of the oxidized outer “rind” of individual grains (e.g. [8]), thereby reducing the effective grain size. Even more cracking occurs during the formation and spallation of U_3O_8 . The original distribution of grain sizes present from the fabrication process, the variable grain growth that occurs due to axial and radial temperature distributions, and the effective reduction in grain size caused by cracking, result in a “log-normal” distribution of grain sizes. Stout et al. [9,10,11] have shown that the rate of oxidation depends inversely upon the grain size. Thus, models for the oxidation of U_4O_9 to U_3O_8 must account for both this “log-normal” distribution of grain sizes and the burnup-dependence of the activation energy to accurately predict the oxidation response of spent fuel in a repository.

RESULTS AND DISCUSSION

KINETIC MODEL OF UO_2 OXIDATION

The basic formulation of the grain size statistical dependence for the oxidation response model has been presented previously by Stout et al. [9,10]. Individual grains are assumed to be cubical and are subdivided into six pyramids with square bases. The scalar magnitude of the height vector, \underline{c} , from the face of the grain to the center is defined as $|\underline{c}|$, the grain half-size. For the first transition, the oxidation of spent fuel has been shown to be diffusion controlled through an increasingly thick product-layer. Thus, the velocity for a multi-grain sized sample at which UO_2 is converted to U_4O_9 is inversely proportional to both the grain half-size and the square root of time. For the second transition ($U_4O_9 \rightarrow U_3O_8$), the product layer spalls or cracks, so that the time duration of the conversion front is inversely proportional to the grain half-size, but directly proportional to time. A brief outline of the methodology followed in the model is presented here. Further details and the model of the first transition can be found in [12].

The temperature-dependent rate of reaction for the $U_4O_9 \rightarrow U_3O_8$ transition, k_{U3O8} , is given as

$$k_{U3O8} = k_{U3O8}^0 \exp(-E_A/RT) \quad (2)$$

where k^0 is the pre-exponential constant, R is the ideal gas constant (8.314 J/mole-K), and T is the absolute temperature. Unlike the previous versions of the model, the present version uses the burnup-dependent activation energy as defined in Equation (1). The scalar function $C(t)|_{t>12.4}$,

which has a value between zero and one, is used to scale the length of vector \underline{c} that has been converted to U_3O_8 from U_4O_9 . When $C(t)$ equals zero, the modeled pyramid is all U_4O_9 , and when $C(t)$ equals one, the pyramid is all U_3O_8 . Originally, the model assumed only grains of one size. In order to include the observation of grain-size distributions, C is allowed to be a function of both time and grain half-size. This reaction for a multi-grain sample can be modeled as

$$dC(t,c)/dt = k_{U3O8}/|c| \quad (3)$$

which, when integrated for $t > t_{2,4}$, yields the expression

$$C(t,c) = (t - t_{2,4}) k_{U3O8}/|c| \quad (4)$$

The extent of reaction, or history, of a sample is most often expressed either as the time-dependent change in O/M ratio or as the volume fraction, $VF(V_{U3O8}/V_{U4O9})$, converted to U_3O_8 . These histories are calculated using the equations

$$\Delta(O/M) = 0.42 + 0.33[3C(t,c) - 3C^2(t,c) + C^3(t,c)] \quad (5)$$

$$VF(t,c) = [3C(t,c) - 3C^2(t,c) + C^3(t,c)] \quad (6)$$

If the history of a grain of monosized UO_2 with a grain half size c_i is denoted by $h(t|c_i)$, and $P(c_i)$ denotes the normalized fractional distribution of grains with that half-size, then the average or expected value of the history of a sample undergoing oxidation from U_4O_9 to U_3O_8 is given by:

$$h(t) = \sum_i h(t|c_i)P(c_i) \quad (7)$$

where $h(t|c_i)$ refers to either the change in O/M ratio or the volume fraction as given in Equations (5) and (6). Although the grain size distribution is “log-normal”, the present model is limited to only four distinct grain size bins, each defined by an average grain half-size and the fraction of grains belonging in this bin.

COMPARISON OF THE MODEL WITH EXPERIMENTAL VALUES

The model was compared with data from two distinct experiments utilizing spent fuel: 1) TGA tests in which small samples (~200 mg) were oxidized and the mass increase was continuously monitored, and 2) ODB tests in which larger samples (5-10 g) were oxidized and the mass increase was measured only intermittently. The initial comparison was made with the TGA data since the samples consisted of single fragments and the burnup of each fragment was estimated based on analyses of each individual sample. The burnup of the dry-bath samples was taken as the rod-averaged burnup of the segment from which the samples originated.

The grain-size distributions were found using an iterative process. A set of four representative grain sizes was selected based on knowledge of the as-irradiated grain sizes providing an upper bound, and the extent of cracking estimated from the published micrographs of Thomas et al. [13,14]. The fraction of each sample in that grain size bin was chosen, the code run and iterations performed, changing the grain sizes and fractions, to give the best fit with the experimental $\Delta(O/M)$ histories. The reported [5] uncertainties of 10-15 kJ/mol in the experimental activation energies were used to further optimize the fitting of the model output with experimental oxidation history curves. As seen in Figure 1, the model was in excellent agreement with the TGA data for most samples. The model was then applied to the ODB data (see Figure 2). Again, the agreement for most samples was excellent.

The oxidation history for the U_4O_9 to U_3O_8 transition for both the TGA and ODB samples usually follows an approximately linear weight gain with time. However, a number of samples exhibited a relatively fast, nonlinear weight gain with time at early times after the plateau. At first, it was hypothesized that these samples contained, for some unknown reason, an unusually high fraction of extremely fine grains, whether due to fabrication, irradiation, or subsequent cracking. Using the iterative approach used to fit the model with the other samples resulted in the need for a very large fraction of grains that were much smaller than observed on these samples.

Upon an in-depth review of the data, it was determined that two of the ODB samples (TP-P2-100 and 104F-100) that exhibited this nonlinear weight gain (see Figure 3) had previously had a hydrated phase, possibly dehydrated schoepite, identified on some samples when examined with X-ray diffraction (XRD) analysis. Schoepite is known to exhibit a fine, needle-like structure on the surface of the affected particles. It was hypothesized that the schoepite acted essentially as “fins” that greatly enhanced the effective surface area, or, equivalently, decreased the effective grain size. Not only could the large surface area created by the schoepite allow for greater oxygen absorption, but the low density, highly oxidized material could rapidly transport this oxygen to the U_4O_9 phase beneath it. If this were the case, then as the fuel oxidizes to U_3O_8 and cracks or spalls from the surface, the effect from the schoepite should decrease. This is observed with both the TGA and dry-bath samples that exhibited the “anomalous” behavior; after some initial transient after the plateau, the oxidation proceeds similar to the other samples. Using this justification, the remaining samples were fit with the model and the agreement was again quite good. XRD is currently being performed on all samples to determine if any hydrated phases can be detected for other samples.

Full details of the experiment-model comparisons are not given, but the reader is referred to the Waste Form Characteristics Report, Sec. 3.2.2 [12]. In summary, both those samples with and without the anomalous behavior were modeled with excellent fits. For those experiments that had no evidence of schoepite, the time histories of $\Delta[O/M]_{U_3O_8}$ were in agreement within 3% of the measurements for both TGA and ODB experiments over a burnup range of 11-48 MWd/kgM. Those samples that had suspected schoepite were also in very good agreement with the experimental results. These fits tended to be about within 5% agreement.

IMPACT ON REPOSITORY DISPOSITION

The worst case scenario is the spent fuel is exposed to moist air, but we shall restrict the reactions to dry air in the present paper. Figure 4 shows the volume fraction histories for constant temperature simulations of 200, 150, and 100°C for sample TP-F-003A. This sample has a rather uniform burnup of 27 MWd/kgM for the grain half-size range 1.0-14 μm ; it is believed to have no hydrated phase. Note that because of the Arrhenius dependence of the reaction on temperature, the reaction to U_3O_8 is complete at about 8000 years if the temperature is a constant 200°C; $2.4\text{e}+6$ years if the temperature is a constant 150°C; and $3.3\text{e}+9$ years if the temperature is a constant 100°C. If the repository were to maintain a constant 150°C after failure of the waste package, only 9% of the fuel would be converted to U_3O_8 after 50,000 years.

It is instructive to consider the oxidation of spent fuel at different burnups. Theoretically, the resistance to U_3O_8 formation increases with increasing burnup, although this remains to be proven. Using these fine grain sizes and a broad range of activation energies, a family of curves over a range of temperatures can be generated for use in performance assessment models. Figure 5 shows the resulting plots of the spent fuel volume fraction history having burnups of 25, 50, and 75 MWd/kgM, assuming average grain half-sizes of 4.0, 0.75, and 0.25 μm , respectively. Assuming a constant temperature of 200°C, the corresponding times for complete conversion to

U_3O_8 are 1.3e3, 5.5e5, and 3.4e8 years, respectively. Figure 6 shows the resulting plots of the spent fuel volume fraction histories of the same data set, except that a constant temperature of 100°C is assumed. The corresponding times for complete conversion to U_3O_8 are 4.3e8, 1.1e8, and 1.0e15 years, respectively.

CONCLUSION

Significant U_3O_8 formation due to dry air oxidation is not expected to occur in a geological repository, provided the maximum temperature does not exceed 150°C, after the spent fuel is exposed to oxygen. This finding is predicted even for high burnup fuels that have undergone restructuring and tend to have rather small UO_2 grains. The exponential temperature dependence of the activation energy for U_3O_8 formation is the dominating mechanism. Additional work is needed to verify the burnup dependence of the activation energy at burnups above about 45 MWd/kg M. The role of hydrated phases on oxidation kinetics must also be studied to verify the present assumptions. Still, the model has been shown to accurately predict the oxidation response of spent fuel to within 5%.

ACKNOWLEDGMENTS

This work was performed under the auspices of the U.S. Department of Energy by Lawrence Livermore National Laboratory under Contract No. W-7405-Eng.48. The input of Dr. Stanley Prussin of the University of California Berkeley for the experimental work is greatly appreciated.

REFERENCES

- [1] Einziger, R.E. and R.V. Strain, "Behavior of Breached Pressurized Water Reactor Spent-Fuel Rods in an Air Atmosphere Between 250 and 360°C", *Nuclear Technology* **75**:82-95(1986).
- [2] Gray, W.J., L.E. Thomas, and R.E. Einziger, *Mat. Res. Soc. Symp.*, **294**: 47 (1993).
- [3] Matzke, H., J. Ottaviani, D. Pellottiero, and J. Rouault, "Oxygen Potential of High Burnup Fast Breeder Oxide Fuel", *Journal of Nuclear Materials* **160**:142-146(1988).
- [4] Walker, C.T., T. Kamesama, S. Kitajima, and M. Kinoshita, "Concerning the microstructural changes that occur at the surface of UO_2 pellets on irradiation to high burnup", *J. Nucl. Mater.* **188**: 73-79 (1992).
- [5] Hanson, B.D. "The Burnup Dependence of Light Water Reactor Spent Fuel Oxidation", PNNL-11929, Pacific Northwest National Laboratory, July 1988.
- [6] McEachern, R.J., J.W. Choi, M. Kolar, W. Long, P. Taylor, and D.D. Wood, "Determination of the activation energy for the formation of U_3O_8 on UO_2 ", *J. Nucl. Mater.*, **249**: 58-69 (1997).
- [7] McEachern, R.J., D.C. Doern, and D.D. Wood, "The effect of rare-earth fission products on the rate of U_3O_8 formation on UO_2 ", *J. Nucl. Mater.* **252**:145-149(1998).
- [8] Thomas, L.F. and R.E. Einziger, "Grain boundary oxidation of pressurized-water reactor spent fuel". *Materials Characterization*. **28**: 149-156 (1992).
- [9] Stout, R. B., H. F. Shaw, and R. E. Einziger (1989). "Statistical model for grain boundary and grain volume oxidation kinetics in UO_2 spent fuel." (UCRL-100859) Livermore, CA: Lawrence Livermore National Laboratory. [NNA.19891031.0015]
- [10] Stout, R.B., E.J. Kansa, R.E. Einziger, H.C. Buchanan, and L.E. Thomas, "Spent fuel waste form characteristics: Grain and fragment size statistical dependence for oxidation response", in *High level radioactive waste management, Proc. 2nd Annual Int. Conf, American Nuclear Soc and Amer. Soc. Civ. Eng., Lagrange Park, IL* **1**:103-111 (1991).
- [11] Stout, R.B. and H. R. Leider, "Waste form characteristics report: Revision 1, UCRL-ID-108314 Version 1.2, Lawrence Livermore National Laboratory (Nov. 1997)
- [12] Stout, R.B. and H. R. Leider, "Waste form characteristics report: Revision 2, UCRL-ID-108314 Version 1.3, Lawrence Livermore National Laboratory (July. 1998)

- [13] Thomas, L.E., O.D. Slagle, and R.E. Einziger, "Nonuniform oxidation of LWR spent fuel in air", J. Nucl. Mater., **184**: 117-126 (1991).
- [14] Thomas, L.E., R.E. Einziger, and R.E. Woodley, "Microstructural examination of oxidized spent PWR fuel by transmission electron microscopy". J. Nucl. Mater. **166**: 243-251 (1989).

TGA 104-01 (305 C)

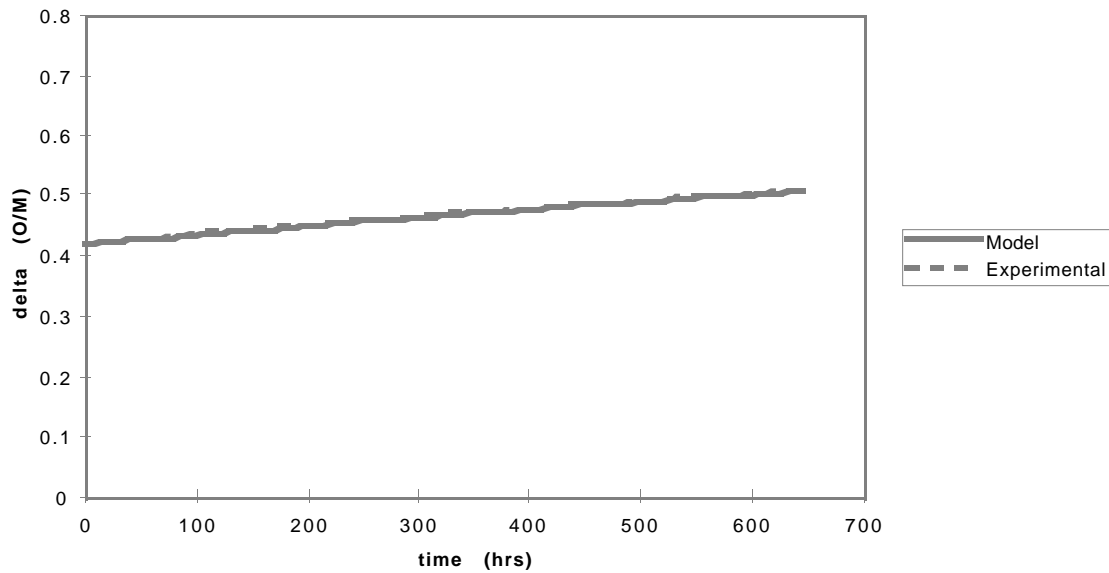


Figure 1. Δ (O/M) versus time (hrs) for the TGA sample ATM 104-01 (305 °C)

ATM 105F-013A

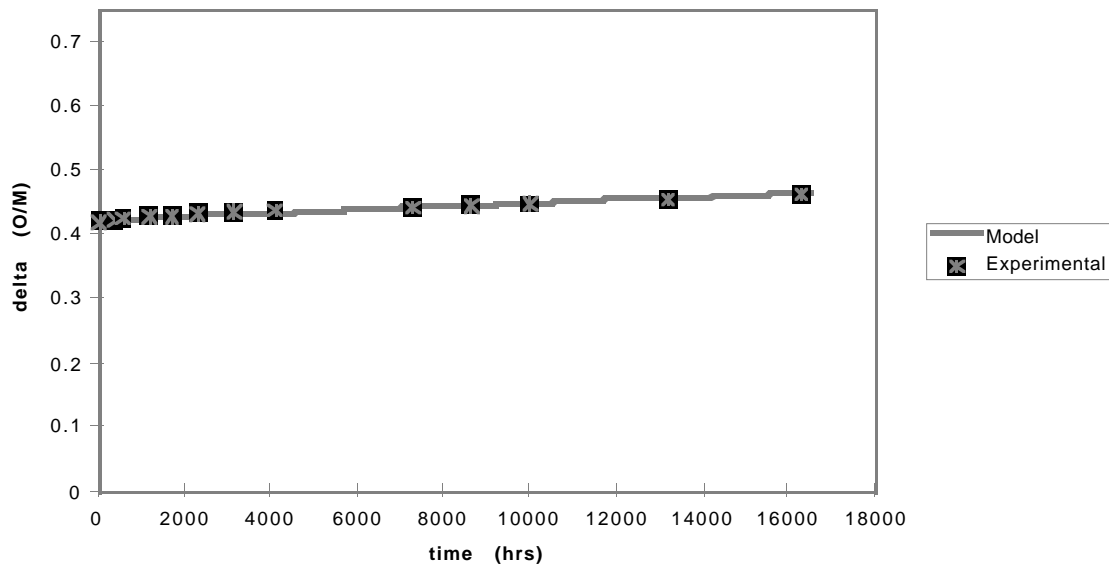


Figure 2. Δ (O/M) ODB experimental and model histories for sample 105F-013A.

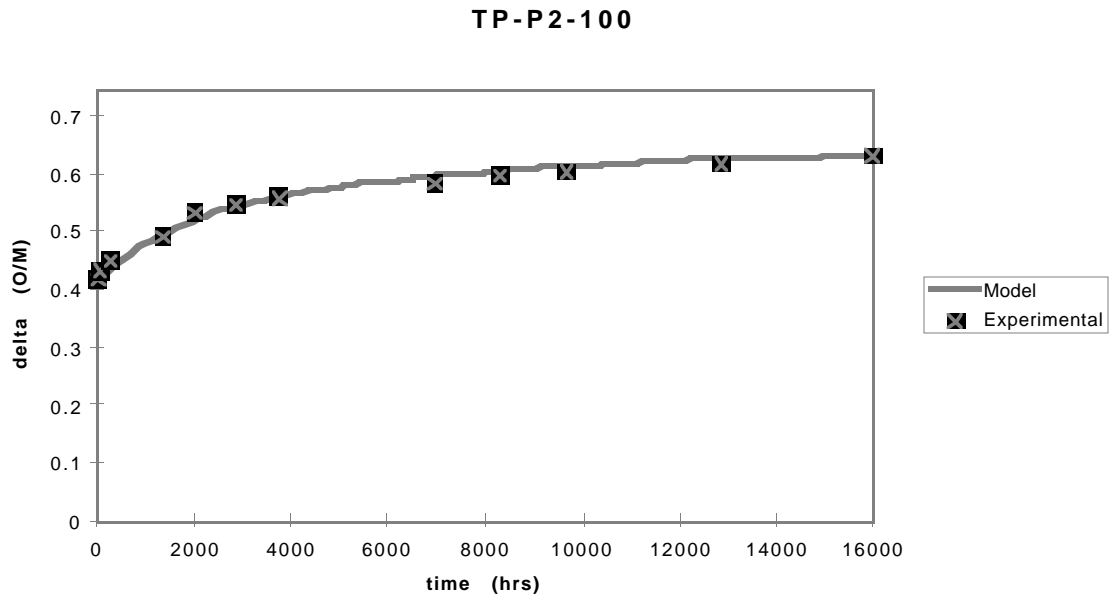


Figure 3. Δ (O/M) versus time (hrs) for the ODB sample TP-P2-100 (255 °C)

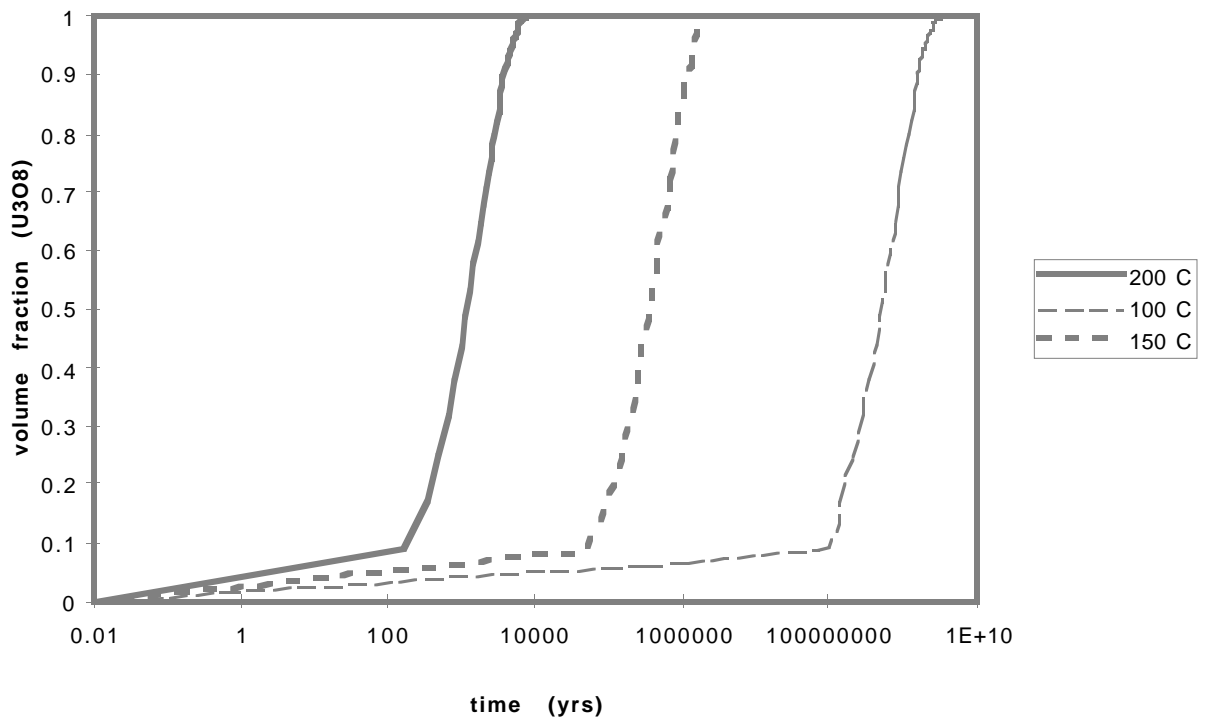


Figure 4. Volume fraction of U_3O_8 formed versus time (yrs) at constant temperature (200, 150, and 100 °C), reference sample TP-F-003A.

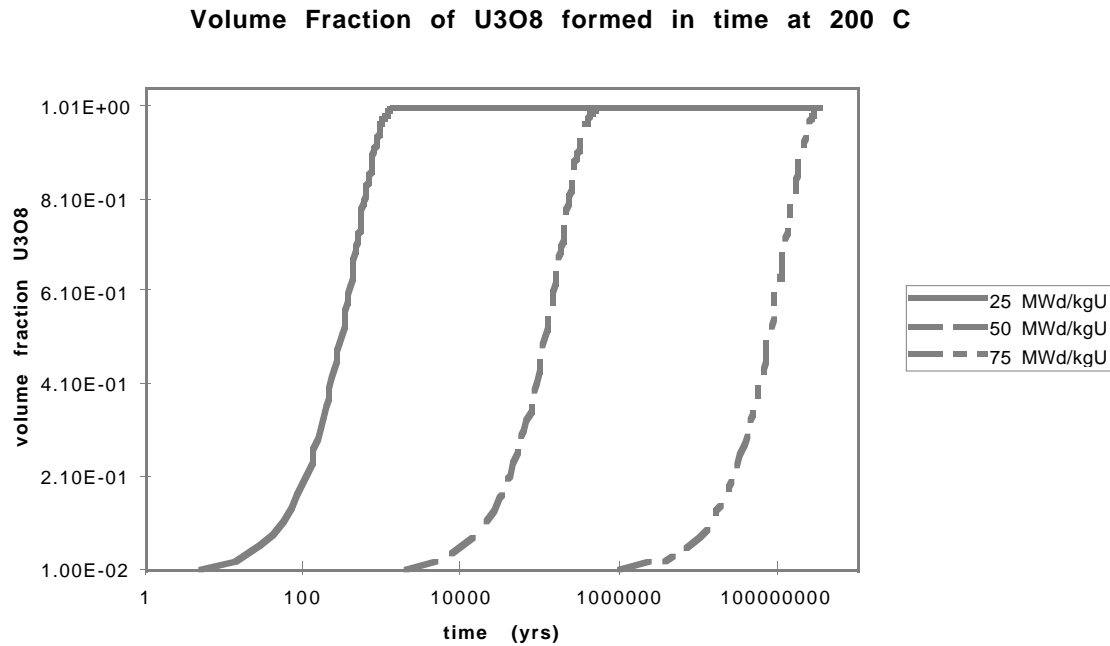


Figure 5. Volume fraction of U₃O₈ formed in time with different burnup fuels at a constant temperature of 200°C, assuming the spent fuel is exposed to oxygen.

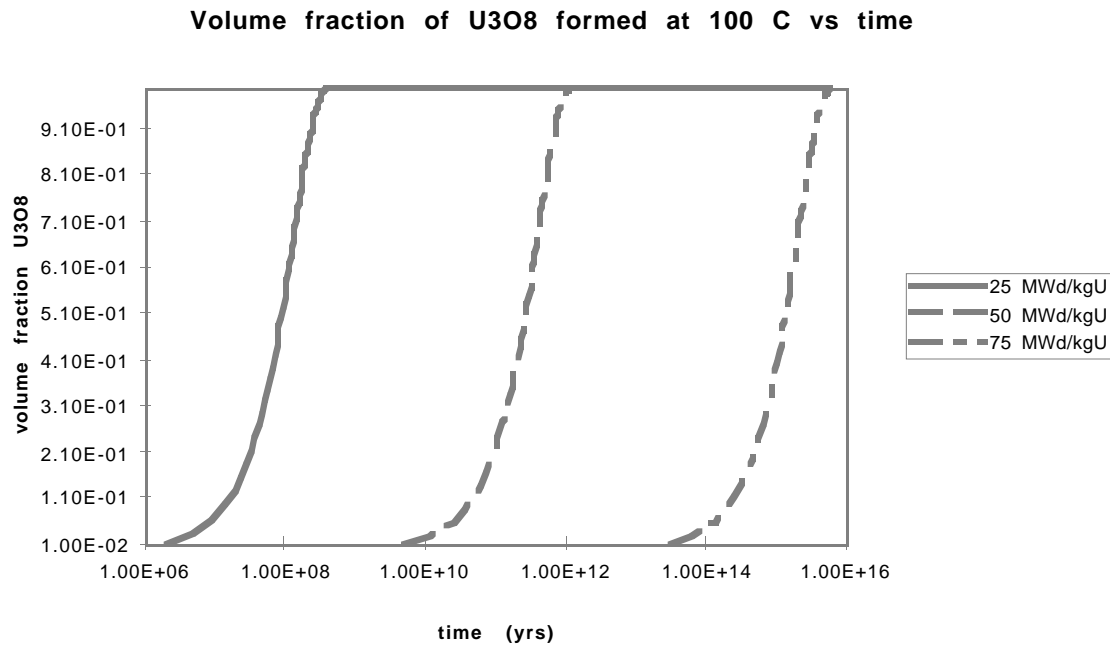


Figure 6. Volume fraction of U₃O₈ formed in time with different burnup fuels at a constant temperature of 100°C, assuming the spent fuel is exposed to oxygen.